Flattening and manipulation of the electronic structure of h-BN/Rh(111) nanomesh upon Sn intercalation

Sugiyama, Yuya ; Bernard, Carlo ; Okuyama, Yuma ; Ideta, Shin-ichiro ; Tanaka, Kiyohisa ; Greber, Thomas ; Hirahara, Toru

Abstract: We have deposited Sn on corrugated hexagonal boron nitride (h-BN) nanomeshs formed on Rh(111) and found that Sn atoms are intercalated between h-BN and Rh, flattening the h-BN. Our reflection high-energy electron diffraction (RHEED) analysis showed that the average in-plane lattice constant of h-BN increases due to the loss of the corrugation. Furthermore, electronic structure measurements based on angle-resolved photoemission spectroscopy (ARPES) showed that the h-BN band width increases significantly while the band width does not change as much. These behaviors were partly different from previous reports on the intercalation of h-BN/Rh system. Our results offer a novel, simple method to control the electronic structure of h-BN.

DOI: https://doi.org/10.1016/j.susc.2018.03.007

Originally published at:
Sugiyama, Yuya; Bernard, Carlo; Okuyama, Yuma; Ideta, Shin-ichiro; Tanaka, Kiyohisa; Greber, Thomas; Hirahara, Toru (2018). Flattening and manipulation of the electronic structure of h-BN/Rh(111) nanomesh upon Sn intercalation. Surface Science, 672-673:33-38.
DOI: https://doi.org/10.1016/j.susc.2018.03.007

Flattening and manipulation of the electronic structure of h-BN/Rh(111) nanomesh upon Sn intercalation

Yuya Sugiyama,[1] Carlo Bernard,[2] Yuma Okuyama,[1] Shin-ichiro Ideta,[3] Kiyohisa Tanaka,[3] Thomas Greber,[2] and Toru Hirahara[1,*]

[1] *Department of Physics, Tokyo Institute of Technology, Tokyo 152-8551, Japan*

[2] *Physik-Institut, Universität Zürich, Winterthurerstrasse 190, CH-8057 Zürich, Switzerland*

[3] *UVSOR Facility, Institute for Molecular Science, Okazaki 444-8585, Japan*

(Dated: March 9, 2018)

Abstract

We have deposited Sn on corrugated hexagonal boron nitride (h-BN) nanomeshs formed on Rh(111) and found that Sn atoms are intercalated between h-BN and Rh, flattening the h-BN. Our reflection high-energy electron diffraction (RHEED) analysis showed that the average in-plane lattice constant of h-BN increases due to the loss of the corrugation. Furthermore, electronic structure measurements based on angle-resolved photoemission spectroscopy (ARPES) showed that the h-BN π band width increases significantly while the σ band width does not change as much. These behaviors were partly different from previous reports on the intercalation of h-BN/Rh system. Our results offer a novel, simple method to control the electronic structure of h-BN.

Keywords: two-dimensional materials; hexagonal boron nitride; intercalation

* hirahara@phys.titech.ac.jp

I. INTRODUCTION

Ever since the discovery of graphene, monatomic-layer-thick two dimensional materials have become one of the hottest topics in condensed matter physics as well as in materials science [1]. Graphene has been mostly employed in the study of Dirac physics [2, 3], and its cousins in group IV, namely silicene, germanene, stanene, have been gaining increased attention [4–7]. However, the presence of a Dirac cone in these systems has been debated extensively since it is believed that the synthesized monolayer interacts strongly with the substrate (see for example, Refs. [8–10] for the case of silicene/Ag(111) and Ref. [11] for the case of stanene/Ag(111)). As a result, the experimentally fabricated systems are quite different from the ideal monolayer films in the theoretical calculations. One solution to overcome this problem is to grow the monolayer sheets on insulating substrates to weaken the film/substrate interaction. For example, it was very recently suggested that stanene grown on PbTe has the expected insulating band gap [12]. Hexagonal boron nitride (h-BN), which is a monolayer sheet of B and N itself with a huge band gap of $\sim$6 eV, is also a promising substrate in this respect. However, h-BN has not been a suitable candidate for practical applications because of the low scalability of the conventional fabrication process of h-BN films, which is the mechanical exfoliation from a small bulk crystals [13].

h-BN films have been successfully grown on substrates such as Ni, Ru or Rh to produce large area samples. Furthermore, a method to produce high-quality h-BN nanomeshs on Rh(111) in wafer scale was developed recently [14, 15]. But these nanomeshes also suffer from the influence of the substrate but several methods are known that can weaken the interaction between h-BN and the substrate [16–19]. Thus further work is needed to make this wafer scale h-BN nanomesh an ideal substrate for material growth. In the present study, we have investigated the effect of Sn deposition on the h-BN/Rh system. We found strong evidence that the deposited Sn is intercalated between h-BN and Rh from our reflection high-energy electron diffraction (RHEED) and angle-resolved photoemission (ARPES) measurements. As a result, the apparent in-plane lattice constant of h-BN increases. Furthermore, we found that the band width of the h-BN σ bands shows small change by the intercalation, whereas the π bands unexpectedly increase their bandwidth by $\sim$0.4 eV. While further investigation is needed to clarify the origin of these changes, our work shows an easy method to control the electronic structure of h-BN.

II. EXPERIMENTAL

The h-BN/Rh(111) samples were prepared as described in Ref. [14]. Briefly, after preparing a single crystal Rh(111) film on yttria-stabilized zirconia (YSZ)-buffered Si(111) [15], h-BN was grown with borazine as the precursor by chemical vapor deposition. The fabricated samples were taken out to air from ultrahigh vacuum (UHV) and the surface was protected with UV-tape protection, cut into pieces and shipped. After removing the protection, the samples were again installed in another UHV chamber. They were then annealed at 550°C for 30 minutes, which resulted in a clear RHEED pattern as shown in Fig. 1(a) that also showed clear spectral features in ARPES measurements (Fig. 2(a)). Sn was deposited on the h-BN/Rh(111) samples at 300°C. 1 monolayer (ML) corresponds to that of the Si(111) surface (7.83×10^{14}atoms/cm^2), which was calibrated by the formation of the Si(111)$\sqrt{3}\times\sqrt{3}$-Sn surface at 1/3 ML deposition onto the Si(111)-7×7 clean surface. While the sticking probability of Sn on the h-BN nanomesh may not be the same as that when deposited on Si(111), we believe that the amount of Sn deposited or intercalated on the h-BN sample should be proportional to the deposition time.

ARPES measurements were performed *in situ* after the sample preparation at BL-5U of UVSOR-III using photons in the energy range of 50-90 eV with p and s polarization. All the data shown were taken at a sample temperature of 30 K. The energy and angular resolutions were 20 meV and 0.25°, respectively.

III. RESULTS AND DISCUSSIONS

Figure 1(a) shows the RHEED pattern after the h-BN/Rh(111) samples were cleaned in UHV. Spots corresponding to the 1×1 periodicity of Rh and h-BN can be clearly seen which are shown by the red and blue arrows, respectively. In addition, numerous spots that correspond to the superstructure periodicity ((13×13) h-BN on (12×12) Rh [20]) can be observed. This is consistent with a previous report which shows the formation of corrugated h-BN nanomesh on Rh(111) [21, 22].

The RHEED patterns of h-BN/Rh(111) changes drastically upon Sn deposition, as shown in Figs. 1(b) and (c) which correspond to samples with 1 ML and 3 ML Sn deposited. One can see that the superstructure spots disappear and the background signal becomes rather

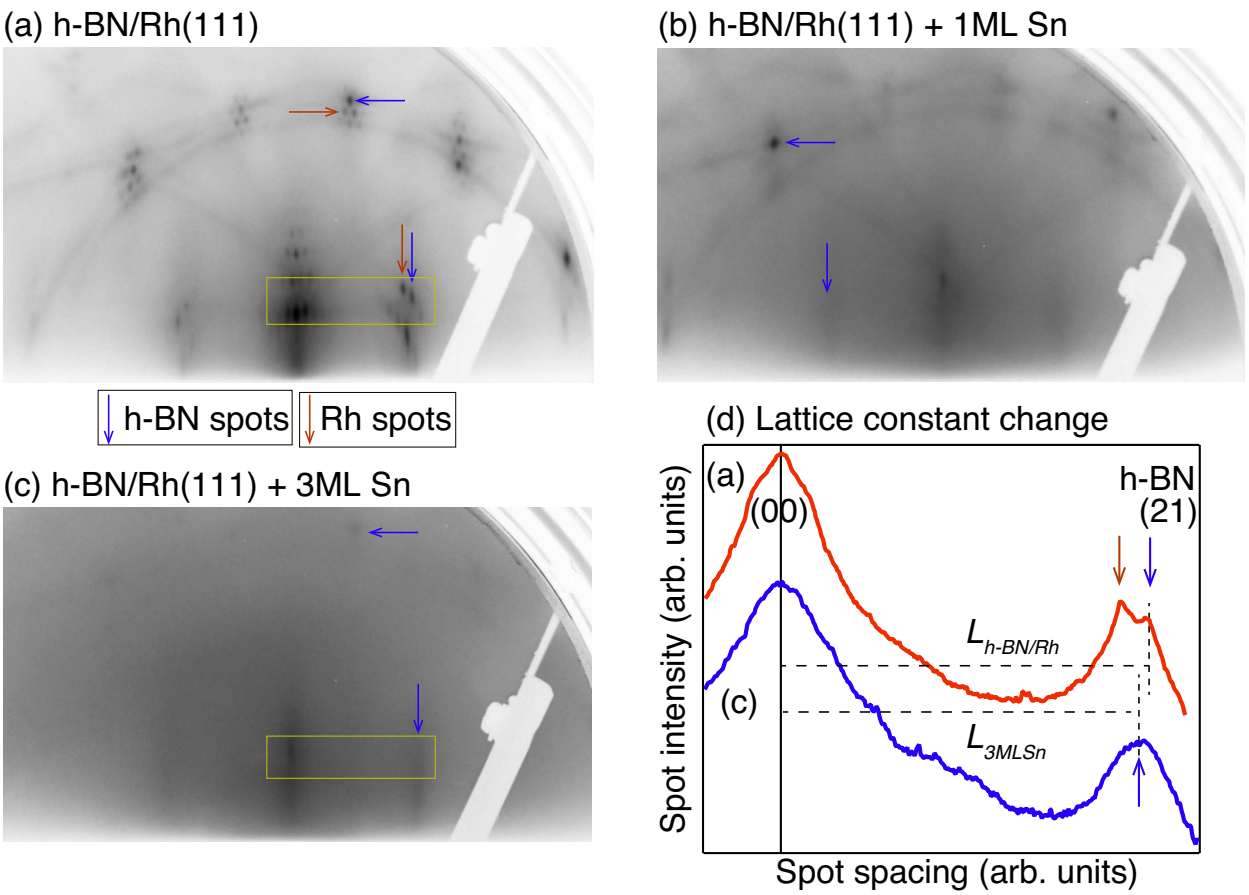

FIG. 1. (a) RHEED pattern of a clean h-BN/Rh(111) sample after annealing in UHV. (b) RHEED pattern of a h-BN/Rh(111) sample after deposition of 1 ML Sn. (c) RHEED pattern of a h-BN/Rh(111) sample after deposition of 3 ML Sn. (d) Line profiles of the rectangular regions in (a) and (c) to show the change in the lattice constant of the h-BN after Sn deposition.

high. Although the 1×1 spots of h-BN is still observed, that of Rh becomes weaker in Fig. 1(b), whereas they completely disappear in Fig. 1(c). Since the Rh spots cannot be seen while h-BN is still present, this seems to suggest that the deposited Sn atoms are not on the surface of h-BN, but are rather intercalated between h-BN and Rh.

We have also investigated the change in the lattice constant after Sn deposition. Figure 1 (d) shows the line profile of the RHEED patterns for the rectangles shown in Figs. 1(a) and (c). It can be seen that the (21) spot of the h-BN has shifted closer to the (00) spot upon Sn deposition. The ratio of the distances is $L_{h-BN/Rh}/L_{3MLSn} \sim 1.02 \pm 0.01$. Since the lattice constant of h-BN/Rh(111) can also be an indication of the corrugation, the expansion of the apparent in-plane lattice constant also suggests that Sn is intercalated between h-BN

and Rh, rendering the h-BN layer closer to freestanding h-BN. Furthermore, since only one ML of Sn is enough to diminish the Rh(111) spots and also make the h-BN spots quite weak, the intercalated Sn layer should be disordered (not an well-ordered layer). In fact, it has been shown that ∼0.6 ML of Sn deposition on Rh(111) leads to the formation of three-dimensional Sn islands in Ref. [23].

To gain further insight about what is happening by depositing Sn on h-BN/Rh(111), we have performed ARPES measurements. Figures 2(a) and (b) show the band dispersion for the clean h-BN/Rh(111) sample taken at a photon energy of $h\nu = 70$ eV with p-polarized photons (a), and $h\nu = 80$ eV with s-polarized photons (b), respectively. To clearly represent the spectral features, the second derivative of the ARPES image is shown. Due to the different symmetry of the σ and π orbitals of h-BN with respect to the mirror plane spanned by the incident photons and the emitted photoelectrons, the photoemission intensity differs significantly by changing the polarization of the incident photons; namely π orbitals that have even symmetry with respect to the scattering plane are detected with p-polarized light, whereas σ orbitals that have both odd and even symmetry can be detected by p and s-polarized light. The photon energies that show the most clear features in the ARPES images have been chosen for each polarization. We note that the band dispersion shown is along the $\bar{\Gamma} - \bar{\mathrm{M}}$ direction. It has been shown that the band width of the π bands along $\bar{\Gamma} - \bar{\mathrm{K}}$ (5.5 eV) is larger than that for the $\bar{\Gamma} - \bar{\mathrm{M}}$ (4.4 eV) from first-principles calculations [24].

Near the Fermi level E_F, one can find multiple bands that originate from Rh in both Figs. 2(a) and (b). In Fig. 2(a), peaks can be found at 8.61 and 9.66 eV that correspond to the π_α and π_β peaks of h-BN, respectively. They represent the electrons at wires and pores of the nanomesh, respectively [18]. Similarly, $\sigma_{\alpha 2}$ and $\sigma_{\beta 2}$ peaks can be found at 4.63 and 5.65 eV in Fig. 2(b). There is also a feature that corresponds to the $\sigma_{\alpha 1}$ band in Fig. 2(a). $\sigma_{\alpha 1}$ and $\sigma_{\alpha 2}$ have different p_x and p_y orbital weights and as a result, show different polarization dependence. Namely, $\sigma_{\alpha 1}$ should have more even-symmetric components with respect to the mirror plane whereas $\sigma_{\alpha 2}$ should have more odd-symmetric components. Such polarization dependence for different σ bands has been reported for graphite [25].

When 1 ML of Sn is deposited(Figs. 2(c) and (d)), one can notice a slight change. First, the $\sigma_{\beta 2}$ band is no longer clearly observed. Moreover, the intensity of the Rh bands as well as the π_β band decrease slightly while that for the π_α and $\sigma_{\alpha 1}$ bands enhance. Further Sn

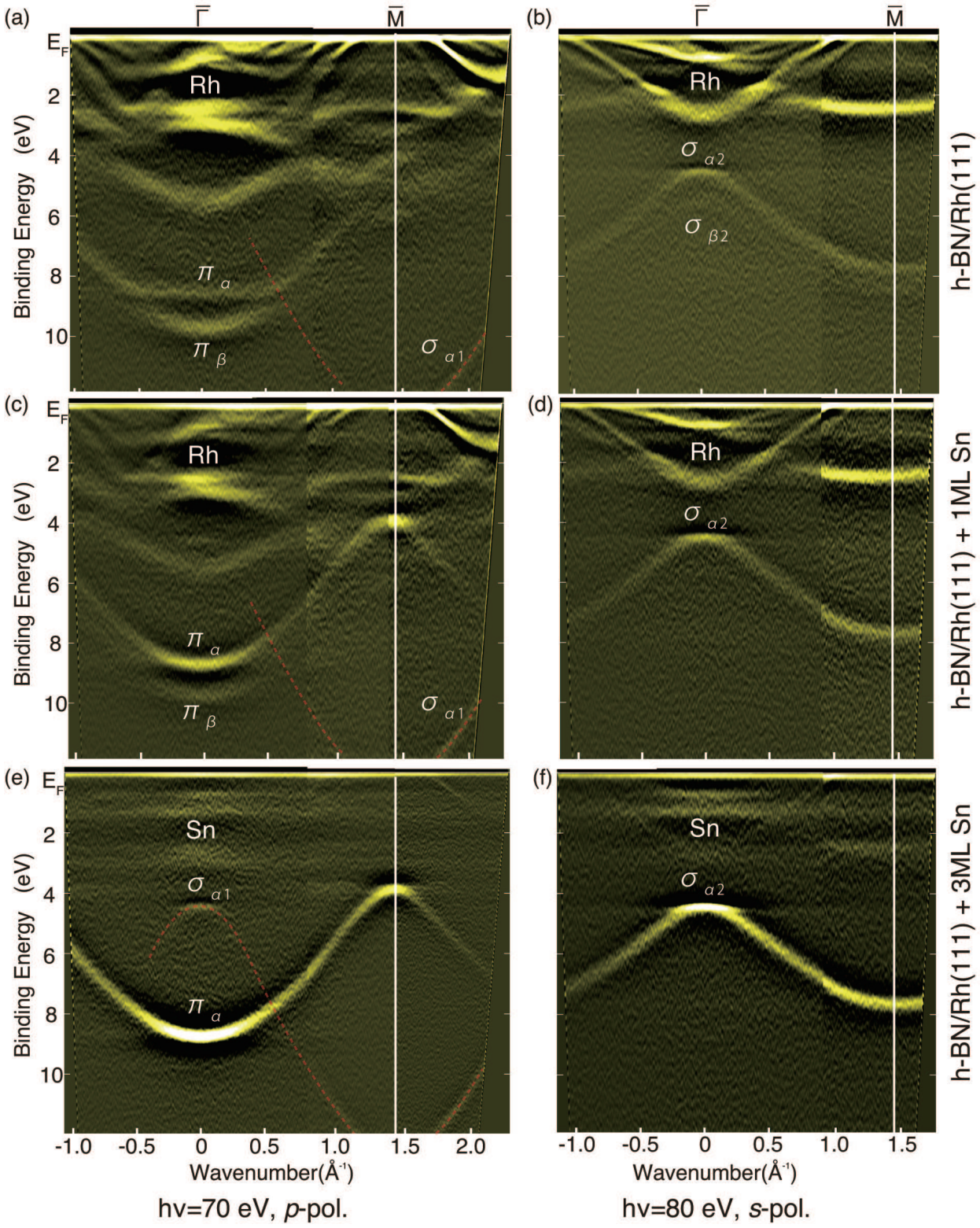

FIG. 2. (a, b) Band dispersion image of a clean h-BN/Rh(111) sample after annealing in UHV. (c, d) Band dispersion image of a h-BN/Rh(111) sample after deposition of 1 ML Sn. (e, f) Band dispersion image of a h-BN/Rh(111) sample after deposition of 3 ML Sn. (a), (c), (e) were taken at $h\nu = 70$ eV with p-polarized photons, while (b), (d), (f) were taken at $h\nu = 80$ eV with s-polarized photons and the dispersion is along the $\bar{\Gamma} - \bar{\mathrm{M}}$ direction.

deposition (3 ML) leads to a loss of the photoelectron intensity for the Rh-derived bands near E_F as well as the π_β band (Figs. 2(e) and (f)). On the contrary, the spectral features of the π_α and $\sigma_{\alpha 2}$ bands become significantly stronger accompanied by an enhancement also for $\sigma_{\alpha 1}$. It can also be noticed that several flat bands appear near E_F which likely originate from the deposited Sn disordered layers. We note that the change in the position of the $\bar{\mathrm{M}}$ point from 1.45 $\mathrm{\AA}^{-1}$ to 1.43 $\mathrm{\AA}^{-1}$ was not clearly observed in contrast to the lattice constant change shown in Fig. 2. This due to the fact that the dispersion was rather flat near the band bottom/top of the σ/ π bands and we only measured the ARPES spectra in 0.25° steps, which roughly corresponds to a change of 0.02 $\mathrm{\AA}^{-1}$.

It has been reported that the loss of the β peaks correspond to flattening of the h-BN nanomesh for the case of H [18] or C intercalation [19]. Our observation suggests that Sn has the same effect as H and C and can be intercalated between Rh and h-BN. The decrease of the Rh state and increase of the h-BN π_α, $\sigma_{\alpha 1}$ and $\sigma_{\alpha 2}$ states in the ARPES spectra also support that Sn is intercalated. This is also consistent with the RHEED observation described above.

We further continue to discuss the quantitative analysis. Figures 3(a) and (b) show the energy distribution curves at the $\bar{\Gamma}$ point for samples with different Sn deposition measured at a photon energy of $h\nu = 70$ eV with p-polarized photons (a), and $h\nu = 80$ eV with s-polarized photons (b), respectively. They are derived from the band dispersion images shown in Fig. 2 and the data for the 2 and 5 ML Sn deposited samples are also included. Figures 3(c) and (d) are the enlarged images of the region surrounded by the dotted rectangles in Figs. 3(a), (b), respectively. One can clearly notice that the peak position of the π_α is shifting to higher binding energy, while the σ_α states shift toward E_F in (d), as indicated by the filled circles. Such energy shift in the peak position of the h-BN states is also found near the $\bar{\mathrm{M}}$ point (Fig. 4). Here both the π_α and $\sigma_{\alpha 2}$ states shift towards the Fermi level.

The energy positions of these peaks are summarized in TABLE I. From this, one can say that all of the states have moved by 100∼200meV. As a result, the bandwidth along the $\bar{\Gamma}-\bar{\mathrm{M}}$ direction of $\sigma_{\alpha 2}$ has become slightly smaller from 2.28 eV to 2.22 eV by 60 meV, whereas that of the π_α increases from 4.46 eV to 4.86 eV by 0.4 eV. This means that the σ band is only slightly altered whereas the π band is affected significantly by the h-BN flattening. The change in the energy position of the the σ states can possibly be ascribed to the change in the work function of the sample (the σ band energy is aligned to the vacuum level, not

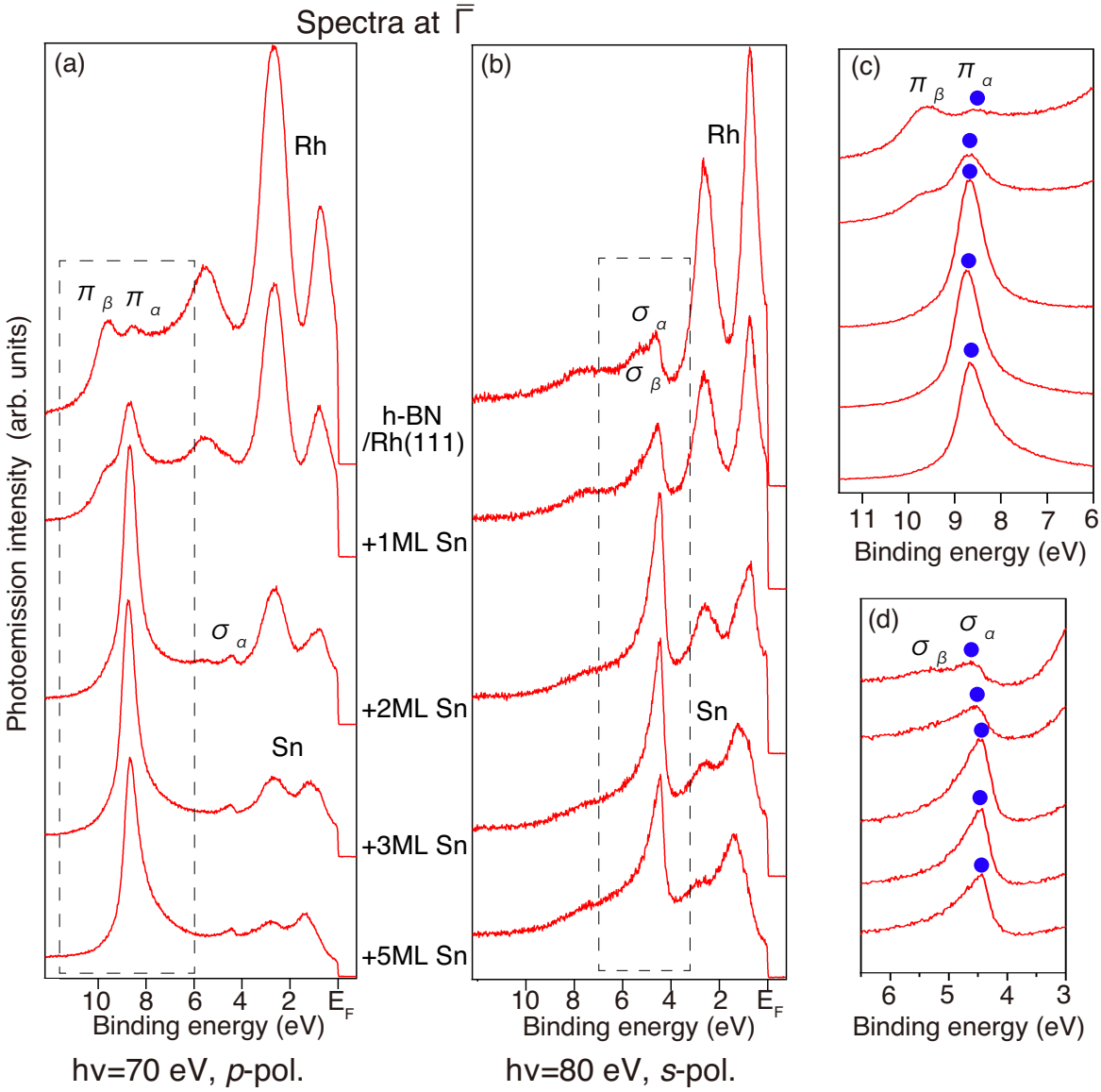

FIG. 3. (a) Energy distribution curves at the $\bar{\Gamma}$ point for the clean h-BN/Rh(111) sample and those with 1-5 ML Sn deposition taken at $h\nu = 70$ eV with p-polarized photons. (b) Same as (a) but taken at $h\nu = 80$ eV with s-polarized photons. (c, d) Close-up of the spectral features in the dotted rectangles in (a) and (b), respectively, showing the change in the peak position.

to the sample Fermi level) as reported in Ref. 26, although we have not actually measured the work function. The enlargement of the π band width can be explained by a change from the wire-pore system to the flat system. Due to the loss of the confinement on the wires of the h-BN nanomesh, electrons can move more freely and have larger dispersion. So this phenomenon can be a general feature for intercalated h-BN/substrate systems, although it

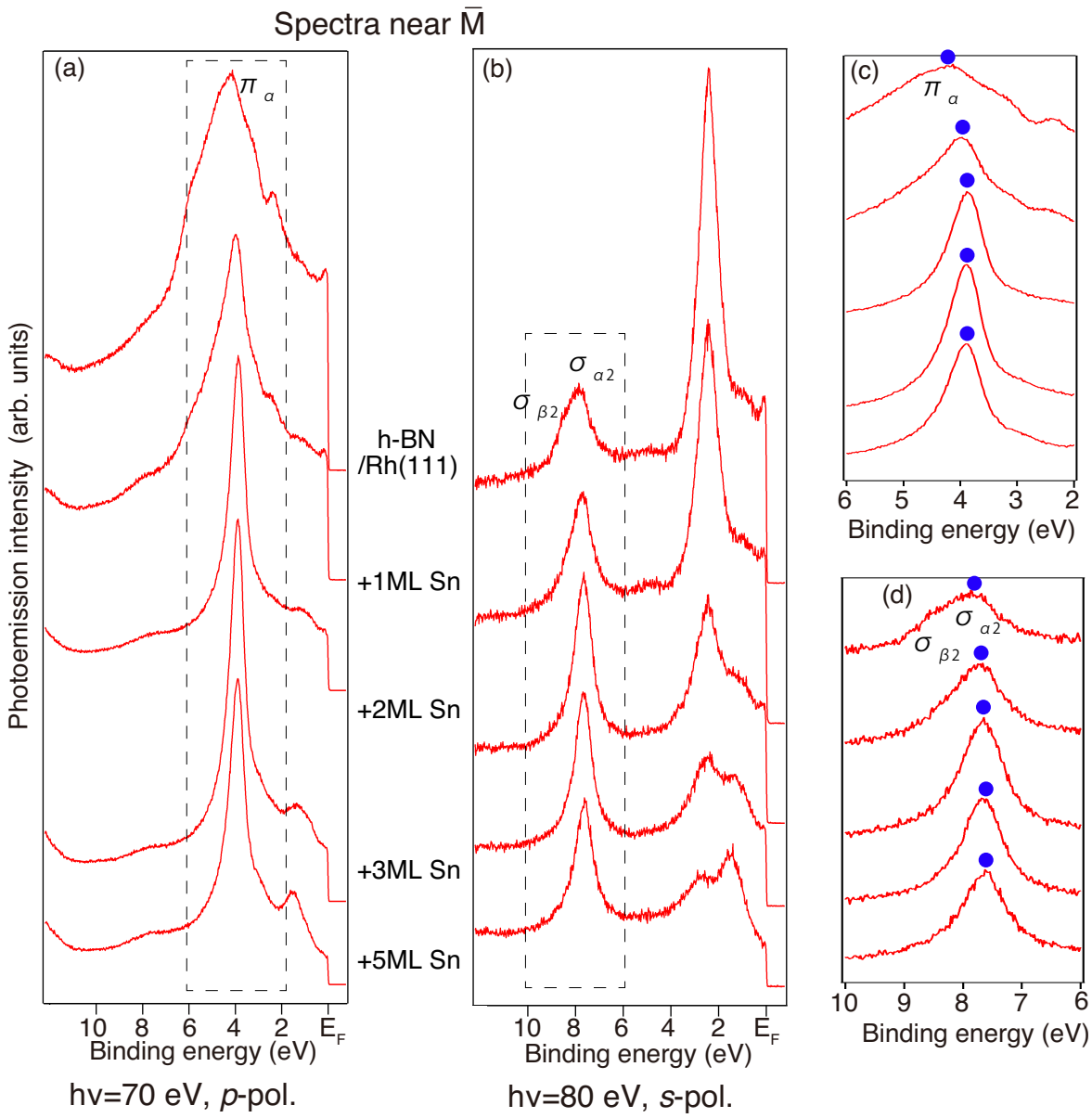

FIG. 4. (a) Energy distribution curves near the $\bar{\text{M}}$ point for the clean h-BN/Rh(111) sample and those with 1-5 ML Sn deposition taken at $h\nu = 70$ eV with p-polarized photons. (b) Same as (a) but taken at $h\nu = 80$ eV with s-polarized photons. (c, d) Close-up of the spectral features in the dotted rectangles in (a) and (b), respectively, showing the change in the peak position.

has never been reported so far.

Now let us compare the present results with the case of H and C intercalation between Rh and h-BN. STM images have clearly shown that the h-BN is flattened by H intercalation [18]. The loss of the π_β and σ_β states was also a clear evidence of the flattening. The

sample	π_α at $\bar{\Gamma}$	σ_α at $\bar{\Gamma}$	π_α at $\bar{\mathrm{M}}$	$\sigma_{\alpha 2}$ at $\bar{\mathrm{M}}$
clean h-BN	8.61	4.63	4.15	7.91
+ 1ML Sn	8.68	4.57	4.00	7.73
+ 2ML Sn	8.69	4.47	3.87	7.67
+ 3ML Sn	8.73	4.45	3.87	7.67
+ 5ML Sn	8.73	4.45	3.87	7.67

TABLE I. Energy positions (eV) of the π_α state at $\bar{\Gamma}$, σ_α state at $\bar{\Gamma}$, π_α state at $\bar{\mathrm{M}}$, and $\sigma_{\alpha 2}$ state at $\bar{\mathrm{M}}$ for different samples.

interesting point is that in this case, no energy shift was observed for π_α and σ_α states, staying at the same energy. Another remarkable point is that the superstructure spots still existed in the diffraction pattern (LEED) after H intercalation despite the flattening [18]. For C, core-level spectroscopy of N 1s showed a clear signature of flattening. Valence band photoemission showed a clear signature of the loss of the β peaks with a shift of the α peaks by 0.5 eV to the higher binding energy side (which was explained as a collapse of the two originally split bands [19]).

The present work of Sn intercalation is partially different from both H and C intercalation cases. While the detailed mechanism that leads to this difference remains elusive, the present results open up a way to control the electronic structure of h-BN/Rh at ease; just by changing the intercalated atom, h-BN can have slightly different electronic states. Since these h-BN/Rh samples can be grown at wafer scale, this may be an advantage in using the h-BN for a substrate to realize novel atomically thick materials that show exotic properties such as silicene [27]. In fact it has already been shown that graphene can be grown on the C-flattened h-BN [19]. It would be interesting to explore the intriguing Dirac physics using such samples.

IV. CONCLUSIONS

In summary, we have successfully flattened h-BN formed on Rh(111) by Sn intercalation. Our RHEED and ARPES results show that the h-BN is decoupled upon Sn deposition. Furthermore, we have found that the h-BN π band width increases significantly while that

of the σ band shows minimal change. While further work is needed to clarify the origin of these change, we have shown a easy way to manipulate the electronic structure of h-BN and they may serve as an ideal substrate for fabricating novel two-dimensional nanomeshs based on group IV elements.

V. ACKNOWLEDGEMENTS

This work has been supported by the Toray Science Foundation. Support by the EC under the Graphene Flagship (contract no. CNET-ICT-604391) is gratefully acknowledged. The ARPES experiments were performed under the UVSOR Proposal No 28-526.

[1] A. H. Castro Neto, F. Guinea, N. M. R. Peres, K. S. Novoselov, and A. K. Geim, Science **81**, 109 (2009).

[2] K. S. Novoselov, A. K. Geim, S. V. Morozov, D. Jiang, M. I. Katsnelson, I. V. Grigorieva, S. V. Dubonos, and A. A. Firsov, Nature **438**, 197 (2005).

[3] Y. Zhang, Y.-W. Tan, H. L. Stormer, and P. Kim, Nature **438**, 201 (2005).

[4] P. Vogt, P. De Padova, C. Quaresima, J. Avila, E. Frantzeskakis, M. C. Asensio, A. Resta, B. Ealet, and G. Le Lay, Phys. Rev. Lett. **108**, 155501 (2012).

[5] A. Fleurence, R. Friedlein, T. Ozaki, H. Kawai, Y. Wang, and Y. Yamada-Takamura, Phys. Rev. Lett. **108**, 245501 (2012).

[6] Y. Fukaya, I. Matsuda, B. Feng, I. Mochizuki, T. Hyodo, and S. Shamoto, 2D Materials **3**, 035019 (2016).

[7] F. Zhu, W. Chen, Y. Xu, C. Gao, D. Guan, C. Liu, D. Qian, S.-C. Zhang, and J. Jia, Nat. Mat. **14**, 1020 (2015).

[8] L. Chen, C.-C. Liu, B. Feng, X. He, P. Cheng, Z. Ding, S. Meng, Y. Yao, and K. Wu, Phys. Rev. Lett. **109**, 056804 (2012).

[9] R. Arafune, C.-L. Lin, R. Nagao, M. Kawai, and N. Takagi, Phys. Rev. Lett. **110**, 229701 (2013).

[10] L. Chen, C.-C. Liu, B. Feng, X. He, P. Cheng, Z. Ding, S. Meng, Y. Yao, and K. Wu, Phys. Rev. Lett. **110**, 229702 (2013).

[11] J. Yuhara, Y. Fujii, K. Nishino, N. Isobe, M. Nakatake, L. Xian, A. Rubio, and G. Le Lay, 2D Mat. **5**, 025002 (2018).

[12] Y. Zang, T. Jiang, Y. Gong, Z. Guan, M. Liao, Z. Li, L. Wang, W. Li, C. Song, D. Zhang, Y. Xu, K. He, X. Ma, S.-C. Zhang, and Q.-K. Xue, arXiv:1711.07035.

[13] K. Watanabe, T. Taniguchi, and H. Kanda, Nat. Mater. **3**, 404 (2004).

[14] A. Hemmi, C. Bernard, H. Cun, S. Roth, M. Klöckner, T. Kälin, M. Weinl, S. Gsell, M. Schreck, J. Osterwalder, and T. Greber, Rev. Sci. Instrum. **85**, 035101 (2014).

[15] S. Gsell, M. Fischer, M. Schreck, and B. Stritzker, Jour. Cryst. Growth **311**, 3731 (2009).

[16] W. Auwärter, M. Muntwiler, T. Greber, J. Osterwalder, Surf. Sci. **511**, 379 (2002).

[17] A. Goriachko, Y. B. He, H. Over, Jour. Phys. Chem. C **112**, 8147 (2008).

[18] T. Brugger, H. Ma, M. Iannuzzi, S. Berner, A. Winkler, J. Hutter, J. Osterwalder, and T. Greber, Angew. Chem. Int. Ed. **49**, 6120 (2010).

[19] S. Roth, T. Greber, and J. Osterwalder, ACS Nano **10**, 11187 (2016).

[20] D. Martoccia, S. A. Pauli, T. Brugger, T. Greber, B. D. Patterson, and P. R. Willmott, Surf. Sci. **604**, L9 (2010).

[21] M. Corso, W. Auwärter, M. Muntwiler, A. Tamai, T. Greber, and J. Osterwalder, Science **303**, 217 (2004).

[22] R. Laskowski and P. Blaha, Jour. Phys.: Cond. Mat. **20**, 064207 (2008).

[23] J. Yuhara, M. Schmid, and P. Varga, Phys. Rev. B **67**, 195407 (2003).

[24] G. B. Grad, P. Blaha, K. Schwarz, W. Auwärter, and T. Greber, Phys. Rev. B **68**, 085404 (2003).

[25] S. K. Mahatha, K. S. R. Menon, Surf. Sci. **606**, 1705 (2012).

[26] A. Nagashima, N. Tejima, Y. Gamou, T. Kawai, and C. Oshima, Phys. Rev. Lett. **75**, 3918 (1995).

[27] Z.-X. Guo, S. Furuya, J.-I. Iwata, and A. Oshiyama, Phys. Rev. B **87**, 235435 (2013).